From Blue Pigment to Green Technology: Properties and Applications of Fungi-Derived Pigment Xylindein

G. Giesbers, M. J. Brodeur, R. C. Van Court, S. C. Robinson, and O. Ostroverkhova

Abstract We overview properties of fungi-derived pigments of interest for artistic and technological applications, with a focus on xylindein, a blue-green spalting pigment produced by *Chlorociboria* species. Optical and electronic properties of xylindein are reviewed, and underlying mechanisms behind its attractive properties (which include enhanced photostability and electronic characteristics) and how they are enabled by the hydroxyl groups in the molecular structure of xylindein are discussed. Potential applications of xylindein as a sustainable material for (opto)-electronic and electrochemical devices which include solar cells, electrochemical transistors, and batteries, are described. The features of xylindein and accompanying challenges depending on the application are outlined, and the outlook is presented.

Keywords Fungi-derived pigments · Organic semiconductors · Organic electronics · Bioelectronics

1 Introduction

1.1 Spalting Fungi and Fungi-Derived Pigments

The art of spalting involves using wood stained by a variety of soft-rotting fungi for decorative and artistic work, such as marquetry, intarsia, and woodturning. Spalted wood is used across the globe, but is mostly documented in Western Europe from around the mid-1400s to the late 1600s. It was particularly used in Italy and Germany for elaborate marquetry works (Fig. 1). Spalting is generally broken down into three categories—white rot (a lightening of the wood area due to decay), zone lines (lines of melanin secreted into the wood to act as a physical

G. Giesbers · M. J. Brodeur · O. Ostroverkhova (✉)
Department of Physics, Oregon State University, Corvallis, OR, USA
e-mail: Oksana.Ostroverkhova@oregonstate.edu

R. C. Van Court · S. C. Robinson
Department of Wood Science and Engineering, Oregon State University, Corvallis, OR, USA

S. K. Deshmukh et al. (eds.), *Fungal Biopolymers and Biocomposites*,
https://doi.org/10.1007/978-981-19-1000-5_17

Fig. 1 Bureau, South Germany, 1560–1570, from the Bilbao Fine Arts Museum. The blue-green stain seen is from xylindein, the pigment produced by soft rotting fungi in the *Chlorociboria* genus

barrier between species), and pigmentation (broadly produced, colorfast pigment that deeply penetrates the wood). There are several commonly used spalting fungi in each category, such as *Trametes versicolor* and *Polyporus brumalis* for white rots, *Xylaria polymorpha* for zone lines, and *Chlorociboria* species and *Scytalidium cuboideum* for bright colors (blue-green and red, respectively). Of particular interest is xylindein, the blue-green pigment produced by *Chlorociboria* species (elf's cup), which has a long history of historic use in Western European artwork, and is favored by today's artisans for the long-lasting, UV stable color (Fig. 2).

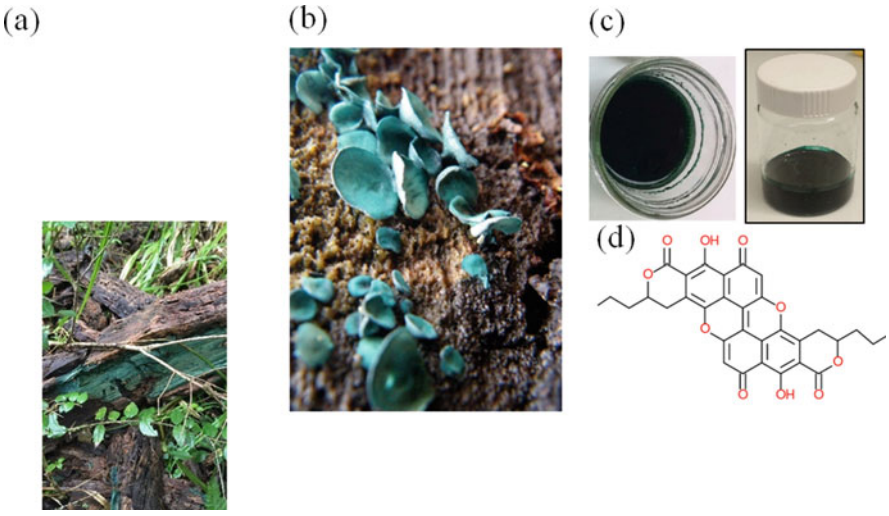

Fig. 2 (**a**) Blue-green stain of *Chlorociboria* on a downed log in Chile, South America. Photo by Dr. Patricia Vega Gutierrez. (**b**) The fruiting cup of *Chlorociboria* spp. on a downed hardwood log in Oregon, USA. Photo by Dr. Seri C. Robinson. (**c**) Xylindein extraction from liquid cultures and pigment in solution. (**d**) Molecular structure of xylindein

In addition to arts and crafts, xylindein has found use in a number of colorant contexts. It has been used as a textile dye (Weber et al. 2014; Hinsch et al. 2015, Fig. 3), decking coating (Vega Gutierrez et al. 2021, Fig. 4), and paint (Robinson et al. 2017, 2018, Fig. 5). Outside of usage as a colorant, over the past ~5 years xylindein has also been investigated as a sustainable (opto)electronic material (Giesbers et al. 2018, 2019a, b, 2021) as discussed extensively in this chapter.

Although the present chapter focuses on xylindein, particularly the mechanisms behind its attractive properties (photostability, enhanced electronic characteristics, and device applications), it is not the only fungi-derived pigment of interest for artistic and technological applications. The orange-red pigment dramada—produced by the spalting fungus *Scytalidium cuboideum*—is a naturally occurring naphthoquinonic crystal (Vega Gutierrez et al. 2018). This pigment has not been as widely studied as xylindein but has been successfully turned into an ink for textile inkjet printing (He et al. 2021, Fig. 6), a decking protectant (Vega Gutierrez et al. 2021, Fig. 4), a paint and oil colorant (Robinson et al. 2017; Robinson et al. 2018, Fig. 5), and has been investigated for hand dyeing of fabrics (Hinsch et al. 2015, Fig. 3). In addition, *Scytalidium ganodermophthorum* produces a range of colors including yellow, green, purple, and red (Vega Gutierrez et al. 2020) which seem to be due to the presence of multiple pigments (Van Court et al. 2020b). The identity of these pigments is so far unknown. Yellow extracts from *S. ganodermophthorum* have shown to produce porous films with morphology similar to those of xylindein (Vega Gutierrez and Robinson 2017) and interesting optical properties (Wiesner 2020). These fungi-derived pigments may have potential for electronic and/or

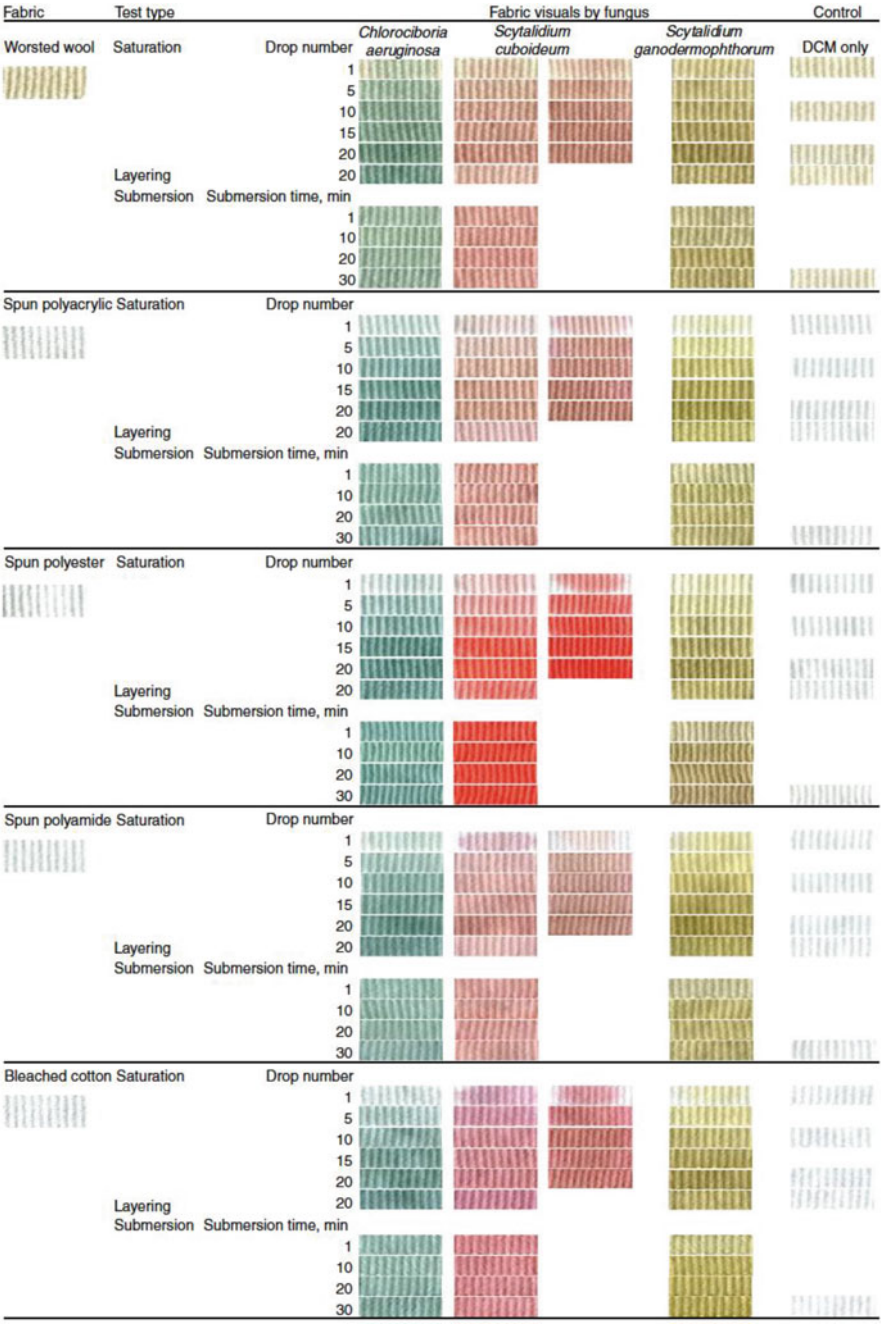

Fig. 3 Extracted pigment from *Chlorociboria* species (blue-green xylindein), *Scytalidium cuboideum* (red dramada), and *Scytalidium ganodermophthorum* (yellow unknown pigment) applied to five different fabric types, showing saturation changes by fabric. Polyester, notoriously difficult to dye, held the most color. From Weber et al. (2014)

Fig. 4 Douglas-fir (*Pseudotsuga menziesii*) and white pine (*Pinus strobus*) wood treated with linseed oil, aniline dyes, or the pigment xylindein (*Chlorociboria* species) / dramada (*Scytalidium cuboideum*) after an accelerated weathering test. The linseed oil mixed with the fungal pigments significantly decreased the cracking and greying of the wood. From Vega Gutierrez et al. (2021)

Fig. 5 Xylindein (blue-green), dramada (red), and the unknown yellow pigment from *Scytalidium ganodermophthorum* can be carried in natural oils, thereby eliminating the need for a solvent carrier. Image shows the color range available. B = xylindein, BR = xylindein + dramada, BY = xylindein + yellow pigment, R = dramada, RY = dramada + yellow pigment, Y = yellow pigment. L = raw linseed oil, D = Danish oil, W = walnut oil

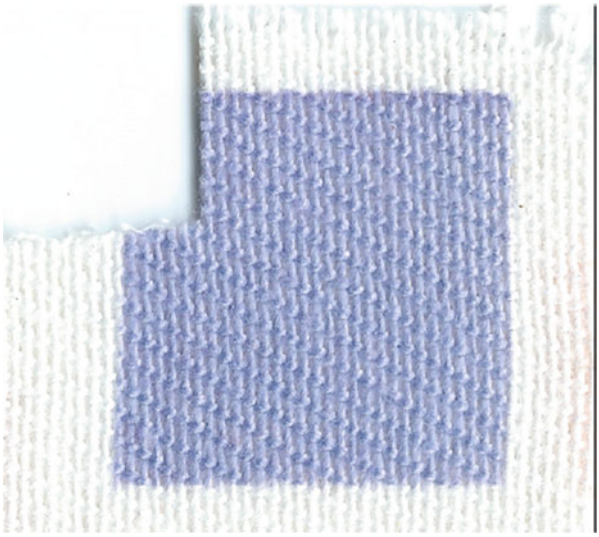

Fig. 6 Dramada (red) pigment from *Scytalidium cuboideum* printed on cotton using an inkjet printer with CTAB-based ink. The pigment was successfully made into an inkjet-compatible ink, which allowed for precise color printing without bleeding edges. From He et al. (2021)

electrochemical applications discussed here in the context of xylindein and require further studies.

1.2 Motivation for Exploring Xylindein as an Organic Semiconductor

There are several technological challenges that humanity must face in the wake of climate change and the need for more sustainable development. Ever since the discovery of conductivity in polyacetylene by Heeger et al. in the 1970s (Shirakawa et al. 1977), organic semiconducting polymers and small-molecule organic materials have been well positioned as a viable replacement for inorganic materials in a variety of (opto)electronic applications (Ostroverkhova 2016). Today, many applications of organic semiconductors have been commercialized, which include organic light-emitting diode (OLED)-based displays and lighting and organic solar cells (Ostroverkhova 2018). The benefits frequently touted are their structural flexibility, ease of processing, and low-cost, to name a few. Organic semiconductor materials that are also sustainable and non-toxic are of special interest.

Many natural products-derived pigments that have been used in art, wood staining, textile dyes, etc. over the centuries (Irimia-Vladu et al. 2011) have a conjugated molecular structure (i.e. containing alternating single and double bonds). However, their utility as organic semiconductors (for which the conventional requirement for the molecular structure is the presence of conjugation) has been limited until recently (Głowacki et al. 2013a, b; Głowacki et al. 2014), although there has been some early work on excited states and charge carrier dynamics in

carotenes (Ehrenfreund et al. 1992) and chlorophyll (Kamat et al. 1986). Even less work has been done on utilizing *fungi-derived* pigments in devices, with only a few reports on using, for example, *Cortinarius* and *Monascus* fungi as sources for sensitizers in dye-sensitized solar cells (Zalas et al. 2015; Ito et al. 2010).Unexpectedly strong performance of naturally derived indigo and other hydrogen (H)-bonded dyes and pigments as organic electronic materials in the past decade has been referred to as a "paradigm shift in molecular electronics design" (Irimia-Vladu 2014). These dyes exhibit high stability with respect to heat degradation and chemical oxidation (which prompts their utility as textile dyes). They also exhibit long-range order and have remarkable photophysical characteristics due to both intra- and intermolecular hydrogen (H-) bonding. Work of Sariciftci and co-workers (Głowacki et al. 2012, 2013a, b, 2014, 2015; Irimia-Vladu et al. 2011; Sytnyk et al. 2014) has documented that H-bonded building blocks, such as indigoids (derived from indigo dye obtained from *Indigofera tinctoria* and *Isatis tinctoria* plants and traditionally used for coloring blue jeans), may contribute good optoelectronic performance, *in spite of lack of intramolecular conjugation,* and stability. These materials owe their performance to intermolecular order that promotes charge delocalization resulting in enhanced charge transport properties that are the key to the electronic device performance. For example, electron and hole mobility of 0.3 $cm^2/(Vs)$ was observed in organic field effect transistors (OFETs) of Tyrian purple, a 6,6′-dibromoindigo pigment originally derived from sea snails and shellfish, and hole mobility of 1.5 $cm^2/(Vs)$ was obtained in epindolidione, a structural isomer of indigo used as a yellow colored toner for printing (Głowacki et al. 2013a, b). Furthermore, power conversion efficiencies of up to 8.2% were obtained from organic solar cells containing indigoids (Deng et al. 2014). Strong (opto)electronic performance of these dyes is coupled with high stability in air (Głowacki et al. 2013a, b); for example, Tyrian purple diode performance showed no signs of degradation even after a month of continuing operation in air, likewise, epindolidione OFET was stable for at least 140 days of operation in air (Gospodinova and Tomšík 2015).

Another high-performance naturally derived building block is H-bonded diketopyrrolopyrrole (DPP) pigments. These are known for their utility in outdoor and automotive paints (e.g. in a famous "Ferrari Red"). However, when used in organic electronic devices, they exhibited ambipolar transport in OFETs with mobilities of up to 0.06 $cm^2/(Vs)$ (Głowacki et al. 2014). Furthermore, DPP-based co-polymers exhibited charge carrier mobilities of >12 $cm^2/(Vs)$, at least four orders of magnitude higher than those in traditional conjugated polymers (e.g. poly (p-phenylene vinylene), or PPV, derivatives) and approaching those in molecular crystals (Ostroverkhova 2016). Finally, some derivatives such as quinacridone (widely used as a magenta colored toner for ink-jet printers) exhibited ambipolar charge carrier mobilities of ~0.1 $cm^2/(Vs)$ (Głowacki et al. 2013a, b) and extraordinarily high photocurrents characterized by an external quantum efficiency (EQE) of 10% in single-component Schottky diodes (i.e. ITO/quinacridone/Al), three orders of magnitude higher than that in similar pentacene (benchmark organic semiconductor) devices (Głowacki et al. 2012).

The work described above served as a motivation to explore H-bonded naturally-occurring spalting fungi-derived pigments as sustainable materials for electronic applications. Xylindein, which exhibits enhanced photostability and high electron mobility (Giesbers et al. 2019a, b), both attractive properties for electronic device applications, is a representative material of this class of promising sustainable organic electronic materials and is the focus of the present chapter. The structure of xylindein was first reported in the 1960s (Blackburn et al. 1962; Edwards and Kale 1965) but its absolute configuration remained unknown for decades, leading to a systematic re-examination in 2000 to obtain the xylindein tautomeric structure (Saikawa et al. 2000). Attempts at xylindein synthesis have so far proven incomplete (Donner et al. 2012), and the work presented in this chapter has been carried out with xylindein extracted from liquid cultures.

The chapter is organized as follows. Section 2 discusses (opto)electronic properties of xylindein and underlying mechanisms. Section 3 introduces challenges that need addressing for viability of xylindein-based electronic devices. Section 4 highlight preliminary work on utilizing xylindein in electrochemical and energy storage devices, and Sect. 5 concludes and presents an outlook.

2 Properties of Xylindein as an (Opto)Electronic Material

2.1 Optical Properties

The important property that motivated exploration of xylindein as an (opto)-electronic material is a rare combination of its enhanced photostability (as compared to conventional organic semiconductor molecules) with promising electronic characteristics (Harrison et al. 2017; Giesbers et al. 2018, 2019a, b, 2021;

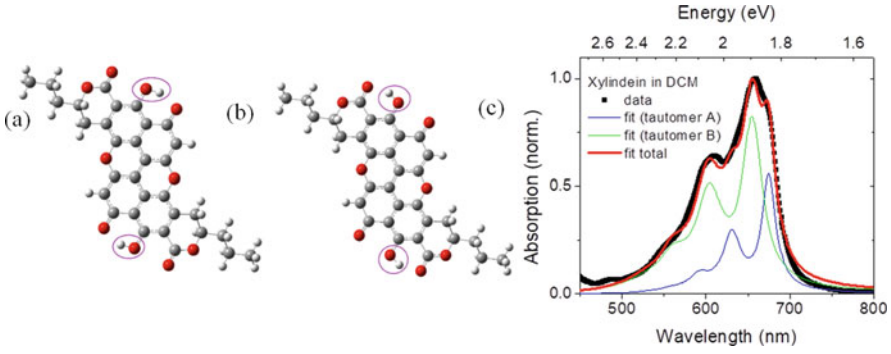

Fig. 7 Molecular structures for xylindein tautomers A (**a**) and B (**b**) with optical properties shown in (**c**). The difference in the orientations of the OH groups between the two tautomers is emphasized by encircling. (**c**) Absorption spectrum of xylindein in dichloromethane (DCM) fit using two vibronic progressions. The sum of the contributions of the two tautomers to the spectra is also included (total fit). From Giesbers et al. (2019a)

Krueger et al. 2021a, b), as summarized in this section. Therefore, for molecular design of next-generation organic electronic materials, it is important not only to characterize the optical and electronic properties of xylindein but also to understand how the molecular structure of xylindein enables these properties.

Optical absorption spectrum of xylindein solution in dichloromethane (DCM) is shown in Fig. 7. The spectrum structure offers an insight into the molecular structure of xylindein and how the molecule interacts with light. In particular, the spectrum exhibits a rather complicated structure that can be described by a sum of two vibronic progressions (Fig. 7). A vibronic progression (a combination of optical transitions offset by a vibrational energy, seen in Fig. 7 as a set of three peaks of varying intensity) is due to the coupling of excitation (electron-hole pair on the photoexcited molecule) to a vibrational mode of the molecule, in this case a C-C stretching mode. The need for two such progressions for properly describing the optical absorption spectrum of xylindein in solution indicates the presence of two dominant tautomers (A and B in Fig. 7) with slightly offset energies of optical transitions (as confirmed by the density functional theory) that contribute to the spectra at a ratio of 30:70 (Giesbers et al. 2019a). Interestingly, these two tautomers exhibit considerable differences in the excited state dynamics, as only one of them undergoes efficient excited-state intramolecular proton transfer (Krueger et al. 2021a). Note that tautomerization of xylindein is related to the OH groups in the xylindein molecular structure; for example, xylindein derivative dimethylxylindein in which the OH groups are replaced by OCH_3 groups does not have tautomers and as a result has a simpler absorption spectrum which fits well with one vibronic progression (Giesbers et al. 2021). The photoluminescence quantum yield of xylindein is low (<0.1%), due to efficient non-radiative decay pathways as discussed in Sect. 3.2.

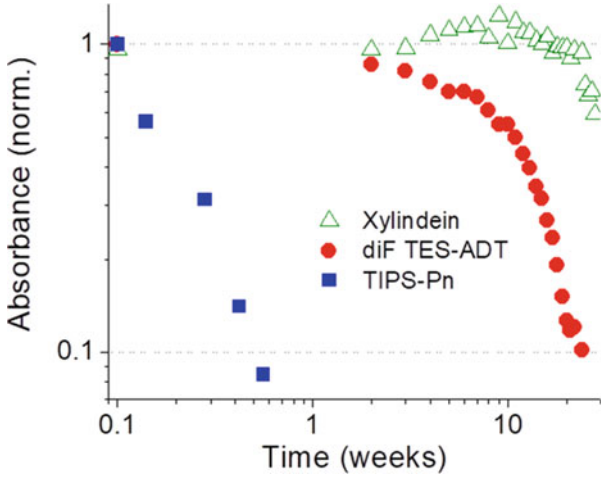

Fig. 8 Integrated optical absorption S_0-S_1 spectra, normalized at time t = 0, of dilute solutions of xylindein and of benchmark organic semiconductors TIPS-Pn and diF TES-ADT continuously illuminated by white light in air, illustrating superior photostability of xylindein in air. From Giesbers et al. (2019a)

2.2 *Photostability*

Figure 8 illustrates that xylindein in solution has a considerably higher photostability as compared to solutions of benchmark organic semiconductors functionalized pentacene (TIPS-Pn) and anthradithiophene (diF TES-ADT) (Ostroverkhova 2016). In particular, under continuous white-light illumination in air, the TIPS-Pn molecules in solution decomposed within 3 days. The fluorinated ADT derivative, diF TES-ADT, which is photostable enough to enable its use as a fluorophore in single-molecule fluorescence spectroscopy (Shepherd et al. 2015), showed a gradual degradation over the period of first several weeks followed by an accelerated degradation starting at about 5 weeks. Under the same illumination conditions, no degradation in optical absorption of xylindein was observed over the period of about 25 weeks, after which partial degradation occurred (Fig. 8) (Giesbers et al. 2019a). In addition, xylindein in solution exhibited enhanced photostability in comparison with other H-bonded pigments, which are known for their enhanced photostability (Yamazaki et al. 2011), including indigo and alizarin (Giesbers et al. 2021). On the molecular level, the photostability of xylindein is enabled by OH groups in its molecular structure and the fast nonradiative excited state processes these groups facilitate such as excited-state intramolecular proton transfer (Sect. 3.2). In particular, a deprotonated xylindein and xylindein derivative where OH groups are replaced by OCH_3 groups (dimethylxylindein), degrade considerably faster than xylindein (Sect. 3.2).

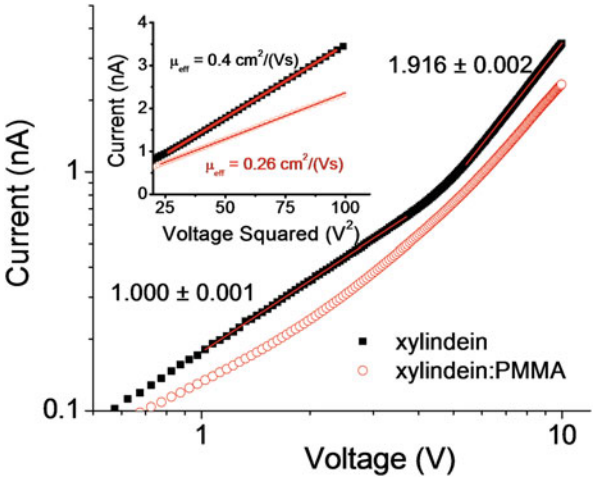

Fig. 9 Current-voltage (I-V) characteristics for pristine xylindein and xylindein:PMMA films on coplanar Al electrodes with a 200 μm gap, exhibiting transition from the linear (Ohmic) to the quadratic (SCLC) regime. Inset shows the current (I) replotted as a function of voltage-squared (V^2) and linear fits slopes of which were used to calculate the effective electron mobilities assuming the thin-film approximation of the SCLCs in the planar electrode geometry. From Giesbers et al. (2019a)

2.3 Electronic Properties

Figure 9 shows current-voltage (I-V) characteristics for a pristine xylindein film on coplanar aluminum (Al) electrodes exhibiting ohmic response followed by a characteristic transition from the linear ($I \sim V$) to the space-charge-limited current (SCLC) ($I \sim V^2$) regime (Day et al. 2009). From SCLC currents (inset of Fig. 9), the values for the effective electron mobility, which is one of the defining characteristics of an electronic material, in the 0.1–0.4 $cm^2/(Vs)$ range were obtained, depending on the device, in pristine xylindein films. These values are considered to be lower bound estimates to the "true", intrinsic value for the electron mobility, as the trap-free SCLC regime (characterized by a sharp, step-like increase in the current at higher voltages, followed by the $I \sim V^2$ behavior but at considerably higher levels of currents) was not reached in these measurements and thus, the intrinsic mobility is higher. Also note that the performance of xylindein-based devices depends on the fungi growth and purification protocols (Van Court et al. 2020a; Giesbers et al. 2019b), and higher mobilities could be possible with improved protocols. Achieving effective mobility values above 0.1 $cm^2/(Vs)$ is rather remarkable given that xylindein films are amorphous, as these values approach the value of ~1 $cm^2/(Vs)$ in amorphous silicon while most amorphous organic semiconductor films have charge carrier mobilities below 10^{-3} $cm^2/(Vs)$. This illustrates benefits of an interplay of intermolecular hydrogen bonding and π-π stacking, made possible by the molecular structure of xylindein but not present in conventional organic semiconductors with molecular structures that lack OH groups and rely only on π-π stacking to promote charge transport. This observation is further supported by four orders of magnitude higher charge carrier mobilities obtained in xylindein films as compared to dimethylxylindein (Giesbers et al. 2021).

As xylindein tends to form porous and inhomogeneous films (Sect. 3.3, Giesbers et al. 2018), in order to improve film processability, blends of xylindein with a polymer polymethylmethacrylate (PMMA) were explored. The PMMA exhibits negligible electric currents in the absence of xylindein, thus providing a non-conductive scaffold for the xylindein molecules (Giesbers et al. 2018, 2019a). The xyindein:PMMA blend yielded considerably smoother films as compared to xylindein films, with optical and electronic properties similar to those of pristine xylindein film (Fig. 9), exhibiting, for example, SCLC effective mobilities of 0.26 $cm^2/(Vs)$ in the xylindein:PMMA film (as compared to 0.4 $cm^2/(Vs)$ in pristine xylindein), inset of Fig. 9. Thus, blending with polymers represents one of the promising routes for improving processability, reproducibility, and performance of xyindein-based films for electronic devices. Blending of xylindein with nature-derived materials such as nanocrystalline cellulose has also been explored (Giesbers et al. 2019a). Although electronic characteristics from these blends were inferior to those from pristine xylindein and xylindein:PMMA blends, this was attributed to non-uniform distribution of xylindein which prevented formation of efficient conductive pathways. This issue could potentially be resolved by improvements in film

processing methods, towards creating a fully nature-derived sustainable organic electronic material.

3 Challenges

3.1 Impurities in Fungi-Derived Pigments and their Effect on the (Opto)Electronic Properties

As spalting is likely a stress response by fungi, pigments are not the only compounds secreted. A host of other compounds (and mycotoxins) are produced both intra and extracellularly by fungi under stress, the makeup of which is not only species specific, but also strain and conditions specific. This mix of secondary metabolites makes purification of xylindein difficult. The preferred solvent for pigment extraction, dichloromethane (DCM),solubilizes other compounds along with xylindein, as seen in high-performance liquid chromatography (HPLC) analysis—most of which are not readily visible to the naked eye and are well hidden in the blue-green extract. While the peaks of such compounds separate out on HPLC, physically removing them has proven difficult (Van Court et al. 2020a; Giesbers et al. 2019b) as illustrated below. As xylindein is produced by many species in the *Chlorociboria* genus, output amount and types of secondary metabolites differ, both across species and within strains (Van Court et al. 2020a). Strain was found to be more important than species in terms of selecting high xylindein output and relative purity (Van Court et al. 2020a). (In contrast, purification of the dramada crystal from *Scytalidium cuboideum* is relatively simple—allowing the DCM solution to evaporate slowly so that the crystals can lengthen. These crystals can then be harvested from the substrate (usually glass) without any competing secondary metabolites (Vega Gutierrez et al. 2018). There also do not appear to be clear strain effects on the amount of dramada produced by *S. cuboideum* (Weber et al. 2016).)

Growth conditions affect metabolite production of all fungi, but are particularly challenging when obtaining pigments from spalting fungi. High nutrient growth conditions lead to mycelial generation but not necessarily to pigment production (Van Court et al. 2020a; Stange et al. 2019), hence conditions must be maintained that stress the fungi without killing them. For cooler-climate fungi, such as *Chlorociboria* species (Richter and Glaeser 2015), this can mean growth at warmer temperatures. For pH sensitive fungi, like *Scytalidium* species, this can mean additions to the growth media to stimulate the desired color output.

Figure 10 illustrates the effect of impurities, most likely secondary metabolites mentioned above, present in xylindein extracted from liquid cultures on the optical properties and electronic characteristics. A simple protocol (“ethanol wash”) was developed to remove some, but not all, impurities, which was observed using mass spectrometry and has manifested into optical and electronic properties (Fig. 10). In particular, Fig.10a, b show a comparison between the absorption and

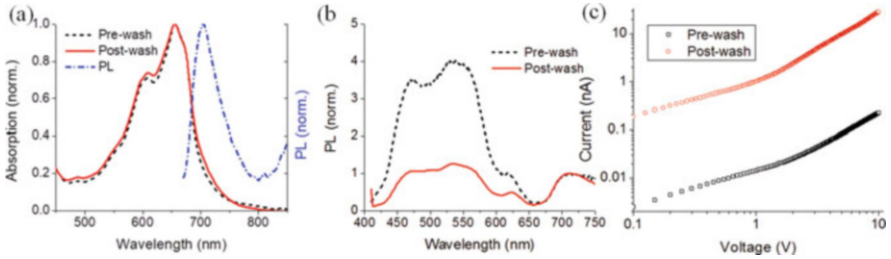

Fig. 10 (**a**) Absorption and (**b**) Emission spectra before and after ethanol wash. In (**b**), PL emission (normalized at its values at 712 nm) was collected with a 400 nm excitation, exhibiting large difference in contribution of contaminants responsible for emission below ~600 nm. (**c**) Current-voltage (I-V) characteristics for the "pre-wash" and "post-wash" xylindein film on coplanar Al electrodes with a 50 μm gap, showing transition from the linear to the quadratic (SCLC) regime. Effective charge carrier mobilities extracted from these SCLC characteristics are 1.6×10^{-3} $cm^2/(Vs)$ for "pre-wash" and 0.19 $cm^2/(Vs)$ for "post-wash" xylindein. From Giesbers et al. (2019b)

photoluminescence (PL) spectra obtained from "pre-wash" (i.e. as extracted) and "post-wash" (i.e. purified using "ethanol wash") xylindein solutions. While the absorption in the 500–700 nm region corresponding to that from the lowest electronic (S_0-S_1) transition of xylindein is preserved (as shown in Fig. 10a), a dramatic reduction in the UV-absorbing species (referred to as contaminants) was observed as a result of the ethanol wash (Giesbers et al. 2019b; Van Court et al. 2020a). The PL of xylindein occurs in the >680 nm wavelength region (Fig. 10a, b) and is weak, characterized by a quantum yield of <0.1%. A considerably stronger PL emission was observed from contaminants in the "pre-wash" sample, occurring in the broad (400–600 nm) spectral region upon 400 nm excitation (Fig. 10b). As seen from Fig. 10b, the ethanol wash substantially reduced the PL emission from the contaminants - by nearly 75% (as compared to the PL emission in the "pre-wash" sample), but it did not eliminate it completely.

Figure 10c shows a comparison between electronic properties of films deposited from "pre-wash" and "post-wash" xylindein solutions. An increase in the electric current (and associated charge carrier mobility) of more than two orders of magnitude was observed in samples made with a "post-wash" xylindein as compared to "pre-wash" xylindein. This large difference in the electronic performance demonstrates importance of development of effective purification protocols for achieving as high purity as possible to boost electronic properties.

Additionally, more than an order of magnitude difference in charge carrier mobility was observed in xylindein films made using xylindein produced by different *Chlorociboria aeruginascens* strains (Van Court et al. 2020a), due to the varying type and concentration of impurities. This further highlights the multitude of variables that could be optimized to achieve the best device performance.

3.2 *Photophysics: High Photostability Versus Photosensitivity for Optoelectronics*

The molecular core of xylindein has a structure of a peri-xanthenoxanthene (PXX). However, the photophysical and electronic properties of xylindein are considerably different from those of unsubstituted PXX and its derivatives studied in the literature, which indicates importance of side groups in xylindein, not present in commonly studied PXX derivatives. For example, xylindein is non-fluorescent (PL quantum yield (QY) of<0.1%), and it favors electron (n-type) transport, in comparison with PL QYs of 0.5–0.97 and hole transport in PXX (Al-Aqar et al. 2017; Kobayashi et al. 2009). Therefore, in order to better understand properties of xylindein and relate them to the specifics of its molecular structure, a molecule with a structure closer to that of xylindein as compared to PXX was necessary. An example of such molecule is a methylated derivative of xylindein (dimethylxylindein), which has most of the features of xylindein's molecular structure except for the OH groups that are substituted with OCH_3 (OMe) groups. A side-by-side comparison of optical and (opto)electronic properties of these two compounds was performed, revealing dramatic differences in their photophysics and (photo)conductivity. In particular, it was demonstrated that the OH groups in xylindein enable processes that are critical both for its remarkable photostability and enhanced electronic properties (Giesbers et al. 2021).

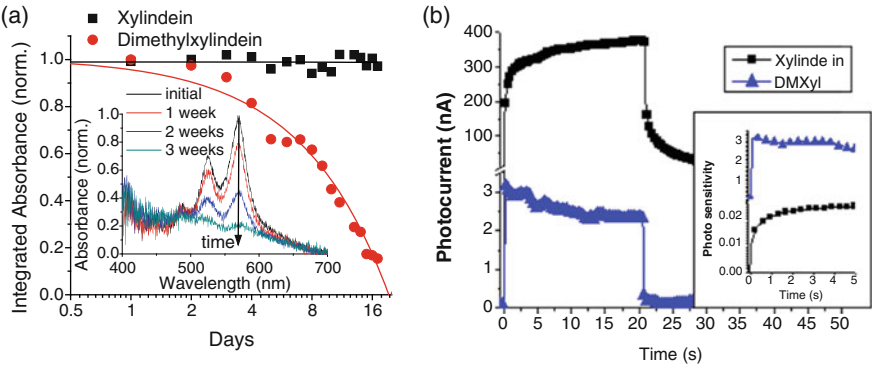

Fig. 11 (**a**) Integrated absorption spectra of xylindein and dimethylxylindein solutions in dichloromethane versus time during exposure to white light in air. Lines provide the guide to the eye. Inset shows time evolution of dimethylxylindein absorption spectra as the compound degrades upon exposure to light. (**b**) Photocurrent from pristine xylindein and dimethylxylindein (DMXyl) films on interdigitated electrodes with a 25 μm gap at the applied voltage of 100 V under 532 nm continuous wave laser illumination turned on at time t = 0 and off after 20 s. Inset shows the photosensitivity of the same films, defined as a ratio of the photocurrent to dark current. Note that although the photocurrent is higher in xylindein (main figure), due to xylindein's superior charge carrier mobility, the photosensitivity is higher in dimethylxylindein (inset), due to dimethylxylindein's more efficient charge photogeneration. From Giesbers et al. (2021)

Figure 11a shows integrated absorption over the S_0-S_1 transition for xylindein (600–700 nm) and dimethylxylindein (520–590 nm) in solution under continuous white light illumination in air. Importantly, dimethylxylindein degraded by more than 80% after only two weeks of exposure, while xylindein showed no evidence of photodegradation under identical illumination conditions during this period of time. Significant photodegradation was also observed in deprotonated xylindein, further demonstrating the importance of the hydroxyl (OH) groups to the photostability of the molecule. Transient absorption spectroscopy (which probes excited-state dynamics on the ultrafast time scales) provides further insight intothe stark difference between the stability of xylindein and dimethylxylindein molecules (Fig. 11a) which revealed fast excited-state decay which depopulates the photoexcited state on picosecond time scales in xylindein as compared to long-lived excited state that persists in dimethylxylindein after many tens of nanoseconds after photoexcitation (Krueger et al. 2021a; Giesbers et al. 2021; Krueger et al. 2021b).

In particular, Fig. 12 shows the potential energy surfaces in xylindein, highlighting efficient ultrafast pathways for energy relaxation both in solution and thin film. In solution (Fig. 12a), fast conformational motions of xylindein lead to a conical intersection (CI) and excited state deactivation on the picosecond time scales, which prevents chemical reactions (such as photo-oxidation) responsible for photodegradation that require a longer-lived excited state.

Figure 11b shows photoconductive properties, important for devices that rely on the ability of materials to generate charge carriers under illumination (e.g. photovoltaic cells or phototransistors), of xylindein and dimethylxylindein films under a 532 nm continuous-wave light excitation. Although the photocurrent is about two orders of magnitude higher in xylindein films than in dimethylxylindein, this is a combined effect of a four orders of magnitude *higher* charge carrier mobility, but two orders of magnitude *lower* charge photogeneration efficiency in xylindein, both of which contribute to the photocurrent resulting in a net higher photocurrent in xylindein. While the higher charge carrier mobility in xylindein is due to a combination of hydrogen bonding promoting intermolecular charge transfer and more favorable film morphology as compared dimethylxylindein, the question arises of why the charge photogeneration efficiency in xylindein is so much lower than that of the dimethylxylindein. The lower photogeneration efficiency in xylindein is illustrated by a comparison of the photosensitivity of xylindein and dimethylxylindein, which is defined as the ratio of photocurrent to dark current. As seen from the inset of Fig. 11b, the photosensitivity was considerably higher in dimethylxylindein. This is due to the differences in the excited state dynamics of these two compounds which are responsible for higher photostability of xylindein (Fig. 11a) but manifest into a lower charge photogeneration efficiency (Fig. 11b) as compared to dimethylxylindein. In particular, as shown in Fig. 12b, c, the photoexcitation of xylindein films is followed by the sub-picosecond excimer formation. This, in turn, is followed by an efficient non-radiative decay which dramatically reduces exciton diffusion lengths which are often necessary for high charge photogeneration efficiency. Therefore, there appears to be a trade-off between photostability and charge photogeneration efficiency in

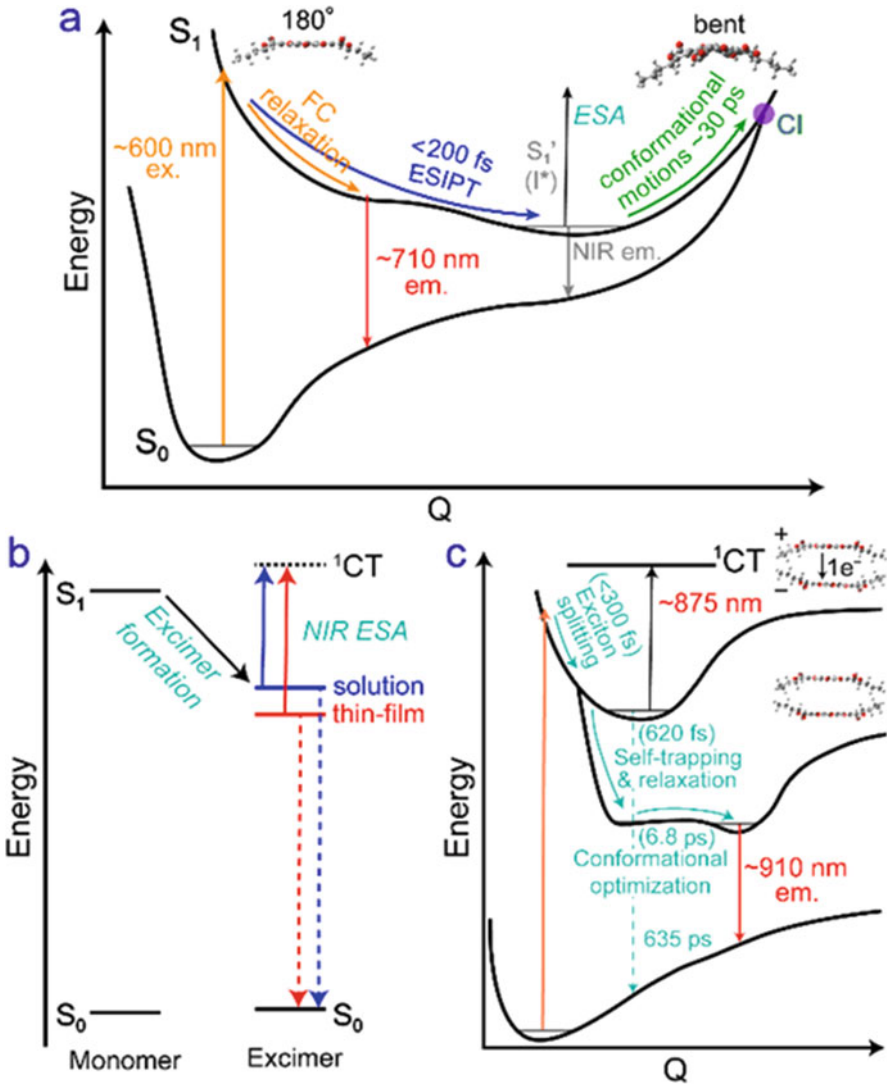

Fig. 12 Potential energy surfaces (PESs) of xylindein in solution and in thin film. (**a**) For xylindein monomer in solution, the insets show the decreasing ring-coplanarity due to conformational motions, which leads to a conical intersection (CI). (**b**) Energy levels for the monomer in solution and for the aggregated solution and thin-film excimers. The excimer to charge-transfer (^{1}CT) absorption band is denoted near-infrared excited-state absorption (NIR ESA). (**c**) PESs of the thin-film xylindein. The excimers following initial structural relaxation exhibit the NIR ESA band to a CT state (Xyl^+-Xyl^-). In (**a**) and (**c**), time constants are listed with their respective dynamic processes. From Krueger et al. (2021a)

xylindein derivatives, which has to be taken into account when optimizing these materials for applications in optoelectronic devices.

3.3 Effect of Morphology

Even though some aspects of pristine xylindein photophysics discussed above are unfavorable for optoelectronic applications, in order to obtain a more comprehensive picture of xylindein as an optoelectronic material, xylindein was investigated as a non-fullerene n-type acceptor material in donor-acceptor (D:A) blends for photovoltaics. This was motivated by the continuing search for more stable n-type organic materials, as current n-type organic semiconductors exhibit low stability with respect to environmental factors (Ostroverkhova 2018; Ostroverkhova 2016). Additionally, the most successful n-type organic materials serving as acceptors in D:A photovoltaics have traditionally been fullerene derivatives that have not only low-stability issues but other unfavorable features including relatively high costs.

In the D:A organic photovoltaics, light excites the donor (p-type organic semiconductor) and/or acceptor (n-type organic semiconductor) and creates a bound electron-hole pair (exciton). The exciton diffuses within the D and/or A domain (which have to have dimensions on the order of exciton diffusion length, typically within ~10 nm) to the D-A interface where it separates, via charge transfer, into free electron and hole charge carriers which then travel to the electrodes and generate the electric current. Initial studies explored potential D:A blends of xylindein with other materials, looking for signatures of charge transfer from the p-type donor molecule to the xylindein acceptor and from xylindein to another acceptor molecule. No signatures of charge transfer states were observed spectroscopically in blends with well-known p-type materials such as poly(3-hexylthiophene-2,5-diyl) (P3HT) and Poly([2,6′-4,8-di(5-ethylhexylthienyl)benzo[1,2-*b*;3,3-*b*]dithiophene]{3-fluoro-2 [(2-ethylhexyl)carbonyl]thieno[3,4-*b*]thiophenediyl})(PTB7-Th) polymers or diF TES-ADT small molecules (Ostroverkhova 2016), or n-type $PC_{60}BM$ fullerene molecule. Thin films of these blends were deposited onto glass substrates with patterned coplanar Au electrodes, excited with a 532 nm light, and the photoconductivity was measured under applied electric field. The blends of P3HT:xylindein and diF TES-ADT:xylindein were less photoconductive than pristine P3HT and diF TES-ADT films, respectively. A PTB7-Th:xylindein blend, however, had a higher photosensitivity (defined as the ratio of photocurrent to dark current) than either pristine PTB7-Th or pristine xylindein (Fig. 13a), thus potentially exhibiting enhanced charge separation at D-A interfaces. This blend was thus chosen to be further investigated in solar cell devices as the active layer, in both conventional (ITO/PEDOT:PSS/active layer/Al) and inverted (ITO/ZnO/active layer/Au) geometry (Giesbers 2021).

Figure 13b shows current-voltage characteristics of solar cells under illumination from a solar simulator with PTB7-Th-only, PTB7-Th:$PC_{60}BM$ and PTB7-Th: xylindein active layers. The control cell with $PC_{60}BM$ acceptor exhibited the

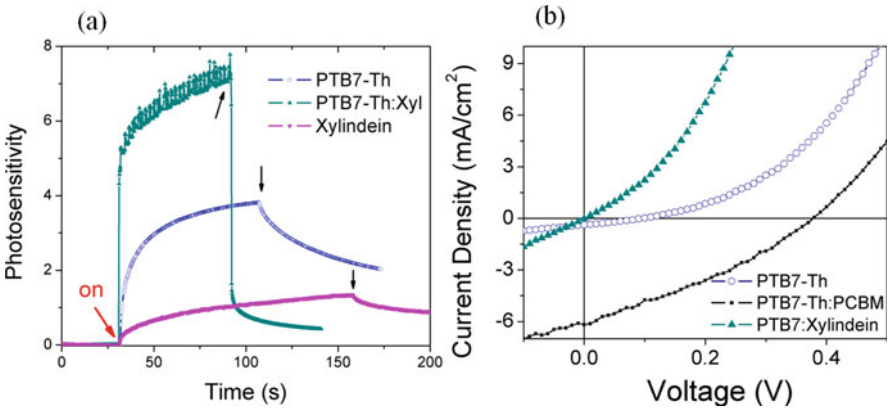

Fig. 13 (**a**) Photosensitivity of thin films of PTB7-Th, xylindein, and a 1:1 w/w PTB7-Th:xylindein blend drop-cast onto interdigitated Au electrodes deposited on glass. Voltage is applied, the white light is turned on at time t = 30 s, and the resulting photocurrent is measured. The arrows indicate the time when the light was turned off. The blend shows an increase in photosensitivity with respect to the pristine materials, indicating its potential as a D/A blend in solar cells. (**b**) I-V curves for organic solar cells under illumination from a solar simulator with PTB7-Th as a donor material. D:A blend of PTB7-Th:xylindein performs not only below benchmark D:A blend PTB7-Th:$PC_{60}BM$ but also below PTB7-Th donor-only solar cells, due to detrimental xylindein morphology for this device geometry

short-circuit current density $J_{SC} \sim 6$ mA/cm^2 and the open-circuit voltage $V_{OC} \sim 0.4$ V, and improvement as compared to pristine PTB7-Th, for which $J_{SC} < 1$ mA/cm^2 and $V_{OC} \sim 0.1$ V were observed. Solar cells with xylindein as an acceptor material, however, had a negligible short-circuit current and open-circuit voltage. In contrast to the enhanced photosensitivity observed in PTB7-Th:xylindein films as compared to both pristine PTB7-Th and xylindein in a planar geometry (i.e. when the film is deposited on the top of the substrate with pre-patterned coplanar electrodes, Fig. 13a), the same blend was not successful in the sandwich configuration (i.e. when the film is placed between top and bottom electrodes) under experimental conditions required by the solar cell operation. In order to investigate the cause of this poor performance in the solar cell with xylindein, ternary blend solar cells were fabricated with PTB7-Th and $PC_{60}BM$ and small amounts (0–5%) of xylindein. These investigations showed that addition of even small amounts of xylindein to the PTB7-Th:$PC_{60}BM$ blend result in a significant decrease in performance, reducing both J_{SC} and V_{OC} (Giesbers 2021).

One important difference between the planar and sandwich geometries and associated experimental conditions for photocurrent measurements is that the latter is considerably more demanding in terms of achieving the optimal film morphology for photoinduced charge separation. In particular, smooth films with the domains on the order of the exciton diffusion length (~10 nm in best-performing organic solar cells) are required. These are difficult to achieve with xylindein which is prone to forming porous structures (Fig. 14) and has a short exciton diffusion length $L_D =$

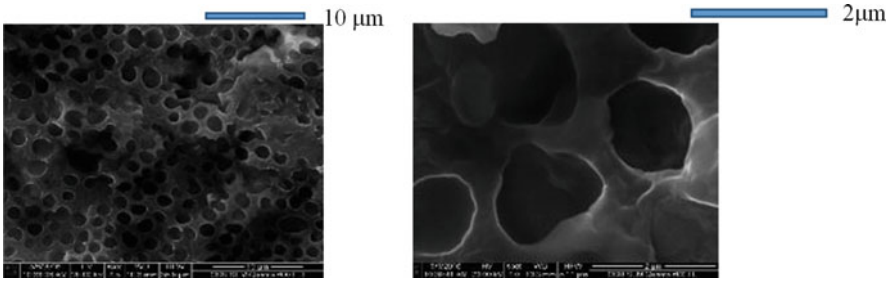

Fig. 14 Scanning electron microscopy images of a drop-cast xylindein film illustrating porous structure of the film (Giesbers et al. 2018)

$\sqrt{D\tau}$, where D is the diffusion coefficient and τ is the exciton lifetime, due to ultra-short exciton lifetimes (Fig. 12). Even though film roughness can be partially mitigated by blending xylindein with polymers (Giesbers et al. 2018), a relatively large polymer fraction is required to achieve film morphology that is suitable for electronic devices in a sandwich geometry such as solar cells (Giesbers et al. 2021), which is detrimental to the electronic properties. The methods for controlling film morphology in xylindein and its derivatives need to be further developed to achieve optimal morphology for applications in solar cells and organic field-effect transistors in which the film quality is critical in order to utilize enhanced electron transport characteristics of xylindein observed in less demanding (i.e. more forgiving with respect to film morphology) device geometries (Sect. 2.3) as compared to those of solar cells and transistors.

In particular, most organic thin-film transistors achieve their best performance when the organic active layer is crystalline (Ostroverkhova 2016). Attempts to apply standard methods of improving film crystallinity (such as substrate surface treatments, thermal and solvent vapor annealing, etc.) developed for conventional organic semiconductors to xylindein have proven unsuccessful, and all xylindein films were amorphous and porous (Fig. 14), regardless of the treatment. This is consistent with the literature (Saikawa et al. 2000) where xylindein crystals were obtained from hot aqueous phenol yielding 4 phenol molecules per xylindein molecule in the asymmetric unit (with the X-ray diffraction-revealed structure yielding a monoclinic space group $P2_1$ with the lattice parameters of a = 8.4 Å, b = 24.0 Å, c = 11.6 Å, and $\beta = 102.2^{\circ}$), but attempts to remove the phenol molecules from crystals resulted in a crystal collapse yielding an amorphous solid. Therefore, routes to xylindein device fabrication with a controlled film morphology and crystallinity require further investigation. Although porous film morphology of Fig. 14 is undesirable for organic solar cells or transistors, it can be beneficial for other applications, for example, energy storage (batteries) which specifically utilize porous materials (e.g. porous titania (Fischer et al. 2017)). Xylindein use in device geometry towards energy storage applications is discussed in Sect. 4.2.

4 Applications

The challenges discussed in the previous section motivated exploration of applications of xylindein in which film quality is less critical. It is known from the literature that hydrogen bonded pigments, exemplified by melanin (another hydroxyl containing naturally occurring pigment), may exhibit protonic conductivity (Vahidzadeh et al. 2018). One signature of this phenomenon is that the conductivity of melanin increases drastically with humidity. It was found that films of xylindein also experience an increase in conductivity in the presence of moisture, which indicates that xylindein too exhibits protonic conductivity, facilitated by the hydroxyl groups. This protonic conduction is a form of ionic conduction. Materials that have significant ionic and electronic conduction have a number of different applications (Surgailis et al. 2021), and only a few have so far been investigated for xylindein, which represents a promising area of research.

4.1 Xylindein for Organic Electrochemical and Water-Gated Transistors

A prominent device application for organic mixed conductors (i.e. materials exhibiting both electronic and ionic conductivity) is an organic electrochemical transistor (OECT) which has been considered to be a building block of biosensors, neuromorphic devices, and complementary circuits (Surgailis et al. 2021). Schematic of OECT geometry is shown in Fig. 15a. First, benchmark OECTs based on poly(3,4-ethylenedioxythiophene) polystyrene sulfonate (PEDOT:PSS) were fabricated. PEDOT:PSS is a conductive polymer mixture that is widely used in the literature and is one of the best performing active materials in OECTs (Rivnay et al. 2018). As expected, the PEDOT:PSS OECT in a conventional geometry (using a 0.1 M NaCl solution as the electrolyte and an Ag/AgCl gate electrode) exhibited a switching behavior in the output characteristics, operating in depletion mode ("on" state with no gate bias and "off" state when positive voltage is applied) (Giesbers 2021). The switching behavior is due to ions from the electrolyte penetrating into the polymer film doping the film. In the case of PEDOT:PSS, which is already p-doped with sulfonate anions from the PSS, the applied gate voltage causes cations to penetrate into the film, negating the doping effects of PSS and decreasing the conductivity of the film (Rivnay et al. 2018). In contrast to well-studied p-type PEDOT:PSS OECTs, xylindein OECT was expected to be a n-type OECT, which are of considerable interest yet face critical challenges and specific requirements for the molecular design (Sun et al. 2018; Giovannitti et al. 2018). When xylindein was tested in the same OECT geometry as PEDOT:PSS, however, the output characteristics were not as expected from an OECT, either p- or n-type (Fig. 15b). Instead, the data exhibited features characteristic of redox activity typically observed using cyclic voltammetry (CV). In particular, the devices (e.g. Figure 15c) exhibited

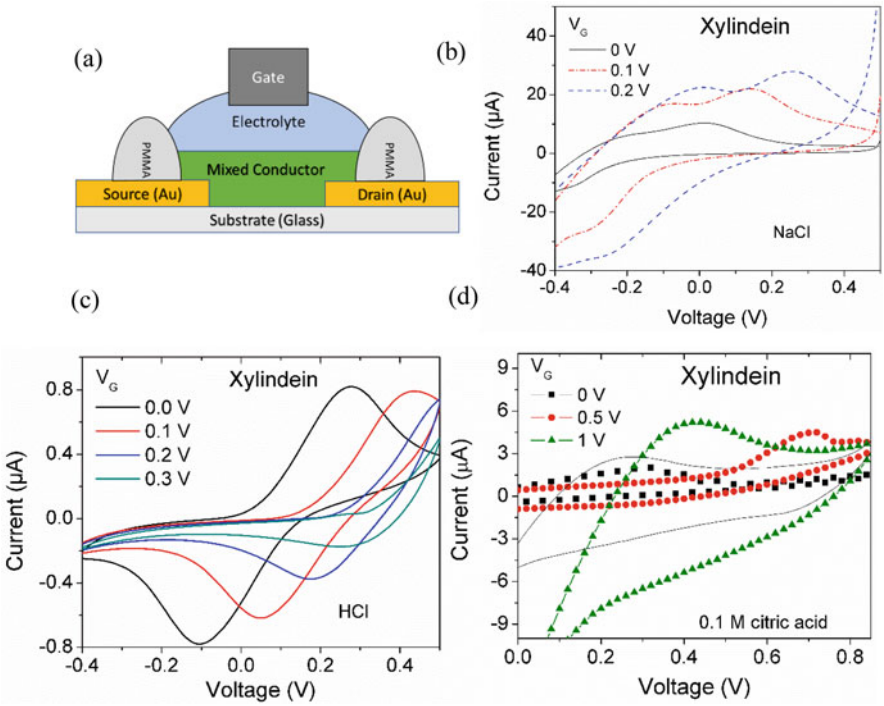

Fig. 15 (**a**) Schematics of OECT configuration. (**b–d**) Cyclic current-voltage sweeps for xylindein devices in an electrochemical transistor configuration with NaCl solution (**b**), 1 mM HCl solution (**c**), or 0.1 M citric acid (**d**) as the gating medium

curves with reduction and oxidation peaks in the classic "duck shape" of CV curves. Several different electrolyte solutions were tested for xylindein devices as a gating medium in a typical OECT configuration of Fig. 15a, each showing redox behavior (NaCl, HCl, and citric acid in Fig. 15b–d). The observed CV-like characteristics are indicative of promising energy storage potential, which will be the focus of Sect. 4.2.

Another class of transistors similar to the OECT is the water gated organic field effect transistor (WGOFET). The configuration of a WGOFET is essentially the same as an OECT, except that deionized (DI) water is used instead of an electrolyte solution in Fig. 15a. The principle of operation of such WGOFETs is that dissolved ions in the water from exposure to air form an electronic double layer when voltage is applied and a field effect occurs in the material (Nguy et al. 2019; Yaman et al. 2014; Porrazzo et al. 2017). Similar to OECTs, the WGOFETs have applications in biotechnology such as biosensors and neuromorphic devices (Rivnay et al. 2018; Cramer et al. 2013). Xylindein is particularly suited to these applications due to its non-toxicity (Almurshidi et al. 2021).

Output characteristics of a xylindein WGOFET are shown in Fig. 16a, exhibiting a n-type response and a relatively large hysteresis. Other xylindein-containing active layers have also been tested such as xylindein:PEIE (Fig. 16b) where PEIE

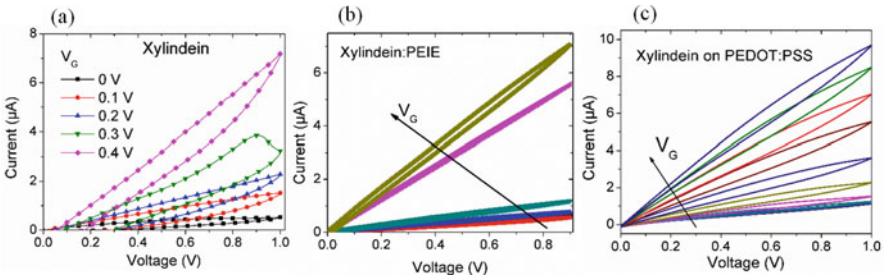

Fig. 16 Output curves from DI water-gated transistors with xylindein (**a**), xylindein:PEIE (**b**) and xylindein on a thin layer of PEDOT:PSS (**c**) as the active layer

(polyethylenimine ethoxylated) is a polymer commonly used as an interface layer material in organic solar cells which promotes charge collection. It also has been successful in blends (such as ZnO:PEIE (Yu et al. 2019)) in enhancing electron transport and serving as an electron transport layer in organic solar cells. Blending xylindein with PEIE almost eliminated the hysteresis seen in pristine xylindein devices, although the currents in both devices were comparable (Fig. 16a, b). Xylindein on PEDOT:PSS (a material widely used in OECTs discussed above) as an active layer in WGOFETs was also explored (Fig. 16c) and yielded higher currents than those in pristine xylindein devices. A figure of merit derived from I-V characteristics of Fig. 16 is transconductance, defined as a ratio of a change in the output current of the device and a change in the applied voltage. The transconductance values were on the order of μA/V, comparable to other WGOFET devices such as those based on a commonly used polymer P3HT (Yaman et al. 2014; Porrazzo et al. 2017). However, the response time for the observed switching behavior in the xylindein WGOFETs was notably slow, on the order of minutes. This would be unexpected for an electronic response such as a field effect, and still many times slower than the response of a typical OECT. Therefore, working mechanism of this device is potentially different from that in both an FET and an OECT which requires further investigation. The slow response in this geometry, however, could be related to an efficient charge storage, which would be advantageous for battery applications, as discussed next.

4.2 Xylindein for Energy Storage Applications

Quinone derivatives, including naturally derived pigments such as melanin and alizarin, have been studied extensively for use in battery applications (Kim et al. 2016; Tong et al. 2019; Luo et al. 2014; Han et al. 2019). There are several considerations that could make xylindein promising for these applications: (1) xylindein is also a quinone derivative; (2) xylindein forms porous films, which may allow ions to penetrate into the film and enhance the surface area for

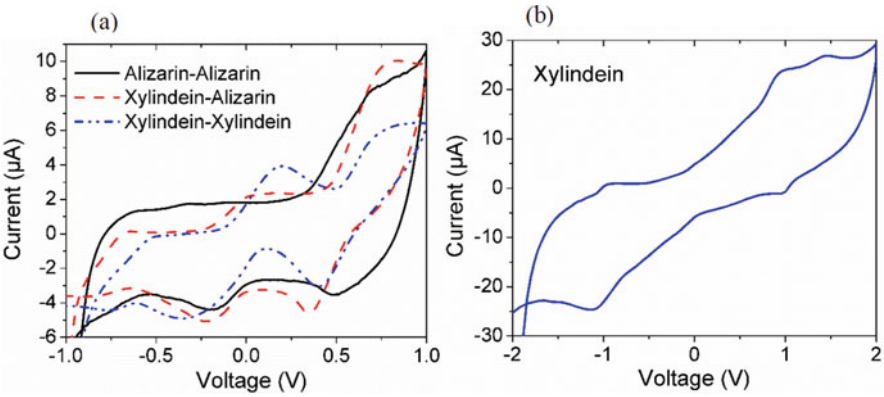

Fig. 17 Cyclic current voltage sweeps for pseudocapacitor devices. (**a**) Sweeps for devices with two alizarin coated electrodes, one alizarin and one xylindein, and two xylindein coated electrodes. Hysteresis indicates charge storage and bumps/dips indicate electrochemical reactions. (**b**) Sweep for the all xylindein device with an expanded voltage window

electrochemical interactions; (3) the redox behavior was observed in xylindein OECT devices, and (4) the slow response time was observed in xylindein WGOFETs discussed in the previous section. Therefore, initial investigation of xylindein-based electrochemical cells was performed in which xylindein was compared to alizarin, a naturally derived hydroxyl groups-containing quinone derivative which has already been demonstrated as a candidate for battery applications (Tong et al. 2019). In this investigation, pseudocapacitor structures were fabricated consisting of two carbon electrodes immersed in a 0.1 M H_2SO_4 solution. The electrodes were coated via drop-casting with either xylindein or alizarin. Figure 17 shows cyclic current-voltage sweeps for the alizarin-alizarin, xylindein-alizarin, and xylindein-xylindein pseudocapacitors. The symmetric alizarin pseudocapacitor (i.e. alizarin-alizarin, with both electrodes coated with alizarin) exhibited two sets of small features due to reduction and oxidation, similar to those reported in the literature (Tong et al. 2019). Similar levels of currents obtained from xylindein pseudocapacitors indicate similar specific capacitance of xylindein-based and alizarin-based devices, which encouraged further exploration. When the voltage window was increased on the symmetric xylindein device (Fig.17b), sets of redox peaks were observed approximately 2 V apart, which is an improvement upon reported alizarin devices (Tong et al. 2019). The wider potential window for xylindein compared to alizarin indicates that there are greater operational limits for the xylindein when compared to alizarin in the same electrolyte, which merits further investigation.

The ongoing research into the development of K^+-ion and Mg-ion battery technology, which are poised to replace Li-ion platforms due to their inherent stability and improved energy density, have not only shown the incorporation of blue pigments (e.g. Prussian blue in the first prototype K^+-ion battery (Eftekhari 2004)), but also the incorporation of quinone compounds as cathode materials within these

next-generation devices (Jian et al. 2016; Dong et al. 2019). The recent literature and promising results of Fig. 17 could position xylindein well as a sustainable option for batteries of the future.

5 Conclusions and Outlook

Investigation into properties of fungi-derived pigment xylindein has provided an insight into mechanisms behind its fascinating optical, photophysical, electrochemical, and electronic properties. Analysis of the optical spectra revealed the presence of two tautomers whose structures and properties were characterized using density functional theory and ultrafast spectroscopy, revealing considerable differences in excited-state dynamics. Excellent photostability was observed in xylindein solutions as compared to those of benchmark organic semiconductor molecules and other hydrogen-bonded pigments. Electron mobility of up to 0.4 cm^2/Vs was obtained in amorphous xylindein films. Xylindein blends with PMMA that feature an improved film morphology and processability, at optimized relative concentrations exhibited (opto)electronic performance comparable to that of pristine xylindein films.

Comparison between optical and (opto)electronic properties of xylindein and those of its methylated derivative, dimethylxylindein has been performed using comprehensive contributions from wood sciences, organic synthesis, ultrafast spectroscopy, quantum chemistry calculations, and device physics. The hydroxyl groups in xylindein, which are not present in dimethylxylindein, were found to play a critical role in optical absorption and photoluminescence properties, excited state dynamics, photostability, and (photo)conductivity. Enhanced photostability of xylindein is attributed to fast deactivation of its excited state; this fast deactivation channel is not as efficient in dimethylxylindein which exhibits a long-lived dark (triplet) state formation instead, which considerably reduces its photostability. At room temperature, amorphous xylindein films were found to be over four orders of magnitude more conductive than both amorphous and crystalline dimethylxylindein films, in part due to differences in charge trap characteristics. The observed large difference in electronic properties of xylindein and dimethylxylindein is partly attributed to the effects of H-bonding in xylindein which promotes morphology supportive of efficient conductive network in xylindein films, in addition to effects of π-π stacking. In contrast to lower electron mobility in dimethylxylindein, the photosensitivity of dimethylxylindein films is considerably higher than that of xylindein films, attributed to higher charge photogeneration efficiency in dimethylxylindein enabled by longer-lived excited states in dimethylxylindein.

Xylindein has proven to have many favorable properties, such as a high stability, relatively high charge carrier mobility in amorphous films, and non-toxicity, for device applications. However, challenges remain to fully utilize these properties. For example, fast excited state deactivation and rough film morphology of xylindein films were found to be detrimental for its use in organic solar cell; the latter is also an obstacle for its applications in organic thin-film transistors. Therefore, better control

of morphology and derivatization to produce xylindein derivatives with more favorable excited state dynamics for applications involving photoinduced charge generation is necessary to address these challenges. The former would require an approach that would counteract poor solubility of xylindein in organic solvents which is detrimental for solution deposition of high-quality films in organic electronic devices. The latter introduces a trade-off as the particular excited state dynamics of xylindein is behind its exceptional photostability, and so any required manipulation of the molecular structure and associated excited states photophysics would most likely decrease the photostability. These issues, however, are not an impediment for certain electrochemical applications (water gated transistors, electrochemical transistors, and batteries), where, for example, the porous morphology of xyindein films could be a feature. Results showing xylindein redox activity in electrochemical device configurations show promise for this type of devices. There are many other potential device applications that are yet to be explored. Similar molecules have been explored for use in fuel cell photocatalysis (Sridharan et al. 2020) and as molecular switches (Früchtl and Van Mourik 2021). Potential bioelectronic applications include biosensors, analytical/diagnostic devices, and neural interfaces (Malliaras 2013). Finally, xylindein is only one example of fungi-derived pigments with properties of interest for sustainable electronics, energy storage, and photonics. Further research is needed to fully understand and harness desirable properties of these fascinating nature-derived materials.

Acknowledgments We thank Profs. C. Fang and C. Beaudry, Drs. J. D. B. Van Schenck and S. Vega Gutierrez, and T. Krueger for their contributions to understanding various aspects of xylindein extraction, characterization, and properties. The authors acknowledge National Science Foundation (CBET-1705099) for financial support.

References

Al-Aqar R, Benniston AC, Harriman A, Perks T (2017) Structural dynamics and barrier crossing observed for a fluorescent o-doped polycyclic aromatic hydrocarbon. Chem Photo Chem 1:198–205

Almurshidi B, Van Court RC, Vega Gutierrez SM, Harper B, Harper S, Robinson SC (2021) Preliminary examination of the toxicity of spalting fungal pigments: a comparison between extraction methods. J, Fungi 7(2):155

Blackburn G, Neilson A, Todd A (1962) Structure of Xylindein. Proc Chem Soc:327–328

Cramer T, Campana A, Leonardi F, Casalini S, Kyndiah A, Murgia M, Biscarini F (2013) Water-gated organic field effect transistors-opportunities for biochemical sensing and extracellular signal transduction. J Mater Chem B 31:3728–3741

Day J, Platt A, Subramanian S, Anthony J, Ostroverkhova O (2009) Influence of organic semiconductor-metal interfaces on the photoresponse of functionalized anthradithiophene thin films. J Appl Phys 105:103703

Deng Y, Liu J, Wang J, Liu L, Li W, Tian H, Zhang X, Xie Z, Geng Y, Wang F (2014) Dithienocarbazole and Isoindigo based amorphous low bandgap conjugated polymers for efficient polymer solar cells. Adv Mater 26(3):471–476

Dong H, Liang Y, Tutusaus O, Mohtadi R, Zhang Y, Hao F, Ya Y (2019) Directing mg-storage chemistry in organic polymers toward high-energy mg batteries. Joule 3:782–793. https://doi.org/10.1016/j.joule.2018.11.022

Donner CD, Cuzzupe AN, Falzon CL, Gill M (2012) Investigations towards the synthesis of Xylindein, a blue-green pigment from the fungus *Chlorociboria aeruginosa*. Tetrahedron 68(13):2799–2805

Edwards RL, Kale N (1965) The structure of Xylindein. Tetrahedron 21(8):2095–2107

Eftekhari A (2004) Potassium secondary cell based on Prussian blue cathode. J Power Sources 126: 221–228. https://doi.org/10.1016/j.jpowsour.2003.08.007

Ehrenfreund E, Moses D, Heeger AJ (1992) Doped Beta-carotene films: Spinless charge storage stabilized by structural relaxation. Chem Phys Lett 196:84–90

Fischer M, Hua X, Wilts B, Gunkel I, Bennett T, Steiner U (2017) Mesoporous Titania microspheres with highly tunable pores as an anode material for lithium ion batteries. ACS Appl Mater Interfaces 9(27):22388–22397

Früchtl H, Van Mourik T (2021) A Quinone based single-molecule switch as building block for molecular electronics. Phys Chem Chem Phys 23(3):1811–1814. https://doi.org/10.1039/d0cp06250b

Giesbers G (2021) (Opto)electronic properties of Xylindein and organic (Opto)electronic devices. Ph. D. Thesis, Oregon State University

Giesbers G, Krueger T, Van Schenck J, Kim R, Van Court RC, Robinson SC, Beaudry C, Fang C, Ostroverkhova O (2021) Role of hydroxyl groups in the photophysics, photostability, and (opto)electronic properties of the fungi-derived pigment xylindein. J Phys Chem C 125:6534–6545

Giesbers G, Krueger T, Van Schenck J, Van Court R, Morré J, Fang C, Robinson SC, Ostroverkhova O (2019a) Fungi-derived xylindein: effect of purity on optical and electronic properties. MRS. Advances 4(31–32):1796–1777. https://doi.org/10.1557/adv.2019.269

Giesbers G, Van Schenck J, Van Court R, Vega Gutierrez SM, Robinson SC, Ostroverkhova O (2019b) Xylindein: naturally produced fungal compound for sustainable (Opto)electronics. ACS Omega 4(8):13309–13318. https://doi.org/10.1021/acsomega.9b01490

Giesbers G, Van Schenck J, Vega Gutierrez SM, Robinson SC, Ostroverkhova O (2018) Fungi-derived pigments for sustainable organic (opto)electronics. MRS Adv 3:3459–3464. https://doi.org/10.1557/adv.2018.446

Giovannitti A, Maria IP, Hanifi D, Donahue MJ, Bryant D, Barth KJ, Makdah BE, Savva A, Moia D, Zetek M, Barnes PRF, Reid OG, Inal S, Rumbles G, Malliaras GG, Nelson J, Rivnay J, McCulloch I (2018) The role of the side chain on the performance of N-type conjugated polymers in aqueous electrolytes. Chem Mater 30(9):2945–2953

Głowacki E, Voss G, Sariciftci N (2013b) 25th anniversary article: Progress in chemistry and applications of functional indigos for organic electronics. Adv Mater 25:6783–6800

Głowacki ED, Coskun H, Blood-Forsythe MA, Monkowius U, Leonat L, Grzybowski M, Gryko D, White MS, Aspuru-Guzik A, Sariciftci NS (2014) Hydrogen-bonded Diketopyrrolopyrrole (DPP) pigments as organic semiconductors. Org Electron 15(12):3521–3528

Głowacki ED, Irimia-Vladu M, Bauer S, Sariciftci NS (2013a) Hydrogen-bonds in molecular solids – from biological systems to organic electronics. J Mater Chem B1(31):3742

Głowacki ED, Leonat L, Irimia-Vladu M, Schwödiauer R, Ullah M, Sitter H, Bauer S, Sariciftci SN (2012) Intermolecular hydrogen-bonded organic semiconductors-quinacridone versus pentacene. Appl Phys Lett 101(2):023305

Głowacki ED, Romanazzi G, Yumusak C, Coskun H, Monkowius U, Voss G, Burian M, Lechner RT, Demitri N, Redhammer GJ, Sünger N (2015) Epindolidiones-versatile and stable hydrogen-bonded pigments for organic field-effect transistors and light-emitting diodes. Adv Funct Mater 25:776–787

Gospodinova N, Tomšík E (2015) Hydrogen-bonding versus π–π stacking in the Design of Organic Semiconductors: from dyes to oligomers. Prog Polym Sci 43:33–47

Han C, Li H, Shi R, Zhang T, Tong J, Li J, Li B (2019) Organic Quinones towards advanced electrochemical energy storage: recent advances and challenges. J Mater Chem A 7:23378–23415. https://doi.org/10.1039/c9ta05252f

Harrison R, Quinn A, Weber G, Johnson B, Rath J, Remcho V, Robinson SC, Ostroverkhova O (2017) Fungi-derived pigments as sustainable organic (opto)electronic materials. Proc SPIE 10101:101010U

He Y, Cao Y, Hwang HJ, Debarajb H, Vega Gutierrez SM, Chen HL, Robinson SC, Malhotra R, Chang CH (2021) Inkjet printing and in-situ crystallization of biopigments for eco-friendly and energy-efficient fabric coloration. In: International Journal of Precision Engineering and Manufacturing-Green Technology, pp 1–13

Hinsch E, Weber G, Chen H-L, Robinson SC (2015) Colorfastness of extracted wood-staining fungal pigments on fabrics –a new potential for textile dyes. J Text Appar Technol Manag 9(3): 1–11

Irimia-Vladu M (2014) Green electronics: biodegradable and biocompatible materials and devices for sustainable future. Chem Soc Rev 43(2):588–610

Irimia-Vladu M, Sariciftci NS, Bauer S (2011) Exotic materials for bio-organic electronics. J Mater Chem 21(5):1350–1361

Ito S, Saitou T, Imahori H, Uehara H, Hasegawa N (2010) Fabrication of dye-sensitized solar cells using natural dye for food pigment: Monascus yellow. Energy Environ Sci 3(7):905

Jian Z, Liang Y, Rodríguez-Pérez I, Yao Y, Ji X (2016) Poly(anthraquinonyl sulfide) cathode for potassium-ion batteries. Electrochem Commun 71:5–8. https://doi.org/10.1016/j.elecom.2016.07.011

Kamat PV, Chauvet JP, Fessenden RW (1986) Semiconductor with a chlorophyll analogue. J Phys Chem 90:1389–1394

Kim YJ, Khetan A, Wu W, Chun SE, Viswanathan V, Whitacre JF, Bettinger CJ (2016) Evidence of porphyrin-like structures in natural melanin pigments using electrochemical fingerprinting. Adv Mater 28(16):3173–3180. https://doi.org/10.1002/adma.201504650

Kobayashi N, Sasaki M, Nomoto K (2009) Stable peri-xanthenoxanthene thin-film transistors with efficient carrier injection. Chem Mater 21:552–556

Krueger T, Giesbers G, Van Court RC, Zhu L, Kim R, Beaudry C, Robinson SC, Ostroverkhova O, Fang C (2021a) Ultrafast dynamics and photoresponse of a fungi-derived pigment xylindein from solution to thin films. Chem Eur J 27:5627–5631. https://doi.org/10.1002/chem.202005155

Krueger T, Tang L, Giesbers G, Van Court RC, Zhu L, Robinson SC, Ostroverkhova O, Fang C (2021b) Ultrafast triplet state formation in a methylated fungi-derived pigment: towards rational molecular design for sustainable optoelectronics. J Phys Chem C 125(31):17565–17572. https://doi.org/10.1021/acs.jpcc.1c06260

Luo W, Allen M, Raju V, Ji X (2014) An organic pigment as a high-performance cathode for sodium-ion batteries. Adv Energy Mater 4(15):1400554

Malliaras GG (2013) Organic bioelectronics: a new era for organic electronics. Biochim Biophys Acta 1830:4286–4287. https://doi.org/10.1016/j.bbagen.2012.10.007

Nguy TP, Hayakawa R, Kilinc V, Petit M, Raimundo JM, Charrier A, Wakayama Y (2019) Stable operation of water-gated organic field-effect transistor depending on channel flatness, electrode metals and surface treatment. Jpn J Appl Phys 58:SDDH02. https://doi.org/10.7567/1347-4065/ab09d2

Ostroverkhova O (2016) Organic optoelectronic materials: mechanisms and applications. Chem Rev 116:13279–13412

Ostroverkhova O (ed) (2018) Handbook of organic materials for electronic and photonic devices (Woodhead publishing series in electronic and optical materials), 2nd edn. Woodhead Publishing

Porrazzo R, Luzio A, Bellani S, Bonacchini GE, Noh YY, Kim YH, Lanzani G, Antognazza MR, Caironi M (2017) Water-gated n-type organic field-effect transistors for complementary integrated circuits operating in an aqueous environment. ACS Omega 2(1):1–10

Richter DL, Glaeser JA (2015) Wood decay by *Chlorociboria aeruginascens* (Nyl.) Kanouse (Helotiales, Leotiaceae) and associated basidiomycete fungi. Int Biodeterior Biodegradation 105:239–244

Rivnay J, Inal S, Salleo A, Owens RM, Berggren M, Malliaras GG (2018) Organic electrochemical transistors. Nat Rev Mater 3:17086

Robinson SC, Vega Gutierrez SM, Cespedes Garcia RA, Iroume N, Vorland NR, Andersen C, de Oliveira Xaxa ID, Kramer OE, Huber ME (2018) Potential for fungal dyes as colorants in oil and acrylic paints. J Coat Technol Res 15(4):845–849

Robinson SC, Vega Gutierrez SM, Cespedes RA, Iroume N, Vorland NR, McClelland A, Huber M, Stanton S (2017) Potential for carrying pigments derived from spalting fungi in natural oils. J Coat Technol Res 14(5):1107–1113

Saikawa Y, Watanabe T, Hashimoto K, Nakata M (2000) Absolute configuration and tautomeric structure of xylindein, a blue–green pigment of *Chlorociboria* species. Phytochemistry 55:237–240

Shepherd W, Grollman R, Robertson A, Paudel K, Hallani R, Loth M, Anthony J, Ostroverkhova O (2015) Single-Molecule Imaging of Organic Semiconductors: toward Nanoscale Insights into Photophysics and Molecular Packing. Chem. Phys. Lett. 629:29–35

Shirakawa H, Louis E, MacDiarmid A, Chiang C, Heeger AJ (1977) Synthesis of Electrically Conducting Organic Polymers: Halogen Derivatives of Polyacetylene, (CH)x. Chem Comm 16: 578–580

Sridharan M, Kamaraj P, Vennila R, Huh YS, Arthanareeswari M (2020) Bio-inspired construction of melanin-like polydopamine-coated CeO_2as a high-performance visible-light-driven photocatalyst for hydrogen production. New J Chem 44(35):15223–15234

Stange S, Steudler S, Delenk H, Werner A, Walther T, Wagenfuhr A (2019) Influence of the nutrients on the biomass and pigment production of *Chlorociboria Aeruginascens*. J Fungi 5(2): 40

Sun H, Gerasimov J, Berggren M, Fabiano S (2018) N-Type organic electrochemical transistors: materials and challenges. J Mater Chem C 6:11778–11784

Surgailis J, Savva A, Druet V, Paulsen B, Wu R, Hamidi-Sakr A, Ohayon D, Nikiforidis G, Chen X, McCulloch I, Rivnay J, Inal S (2021) Mixed conduction in an N-type organic semiconductor in the absence of hydrophilic side-chains. Adv Funct Mater 31:2010165

Sytnyk M, Glowacki ED, Yakunin S, Voss G, Scho W, Kriegner D, Stangl J, Trotta R, Gollner C, Tollabimazraehno S et al (2014) Hydrogen-bonded organic semiconductor micro- and nanocrystals: from colloidal syntheses to (Opto-)electronic devices. J Am Chem Soc 136(47): 16522–16533

Tong L, Jing Y, Gordon RG, Aziz MJ (2019) Symmetric all-quinone aqueous battery. ACS Appl Energy Mater 2(6):4016–4021

Vahidzadeh E, Kalra AP, Shankar K (2018) Melanin-based electronics: from proton conductors to photovoltaics and beyond. Biosens Bioelectron 122:127–139

Van Court R, Giesbers G, Ostroverkhova O, Robinson SC (2020a) Optimizing xylindein from *Chlorociboria* spp. for (opto)electronic applications. *Processes* 8:1477. https://doi.org/10.3390/pr8111477

Van Court R, Vega Gutierrez P, Robinson SC (2020b) Exploration of Pigment Production by Spalting Fungi *Scytalidium ganodermophthorum* and potential for industry. In: IRG51 Scientific Conference on Wood Protection. International Research Group on Wood Protection. IRG Secretariat. IRG/WP 20-10957

Vega Gutierrez S, Robinson SC (2017) Microscopic analysis of pigments extracted from spalting fungi. J Fungi 3:15

Vega Gutierrez SM, Hazell KK, Simonsen J, Robinson SC (2018) Description of a novel naphthoquinonic crystal produced by the fungus *Scytalidium cuboideum*. Molecules 23(8):1905

Vega Gutierrez P, Almurshidi B, Huber M, Andersen C, Van Court RC, Robinson SC (2020) Expanding the spalting palette: developing yellow, purple, and green pigments from

Scytalidium ganodermophthorum for artistic applications. Int Wood Prod J. https://doi.org/10.1080/20426445.2020.1780543

Vega Gutierrez SM, Stone DW, He R, Vega Gutierrez PT, Walsh ZM, Robinson SC (2021) Red pigment from the fungus *Scytalidium cuboideum*helps prevent 'greying' in decking and other outdoor wood products. Coatings 11:511

Weber G, Chen HL, Hinsch E, Freitas S, Robinson SC (2014) Pigments extracted from the wood-staining fungi *Chlorociboria aeruginosa, Scytalidium cuboideum*, and *S. Ganodermophthorum*show potential for use as textile dyes. Color Technol 130(6):445–452

Weber G, Boonloed A, Naas K, Koesdjojo M, Remcho V, Robinson S (2016) A method to stimulate production of extracellular pigments from wood-degrading fungi using a water carrier. Curr Res Environ Appl Mycol 6(3):218–230

Wiesner C (2020) Optoelectronic properties of a novel fungi-derived pigment. B. Sc. thesis, Oregon State University

Yaman B, Terkesli I, Turksoy KM, Sanyal A, Mutlu S (2014) Fabrication of a planar water gated organic field effect transistor using a hydrophilic polythiophene for improved digital inverter performance. Org Electron 15(3):646–653. https://doi.org/10.1016/j.orgel.2013.12.024

Yamazaki S, Sobolewski A, Domcke W (2011) Molecular mechanisms of the photostability of indigo. Phys Chem Chem Phys 13:1618–1628

Yu H, Huang X, Huang C (2019) PEIE doped ZnO as a tunable cathode interlayer for efficient polymer solar cells. Appl Surf Sci 470:318–330

Zalas M, Gierczyk B, Bogacki H, Schroeder G (2015) The Cortinarius Fungi Dyes as Sensitizers in Dye-Sensitized Solar Cells. Int J Photoenerg 2015:653740